Article

Self-Organization of a Self-Assembled Supramolecular Rectangle, Square, and Three-Dimensional Cage on Au(111) Surfaces

Qun-Hui Yuan, Li-Jun Wan, Hershel Jude, and Peter J. Stang

J. Am. Chem. Soc., **2005**, 127 (46), 16279-16286• DOI: 10.1021/ja0549300 • Publication Date (Web): 28 October 2005

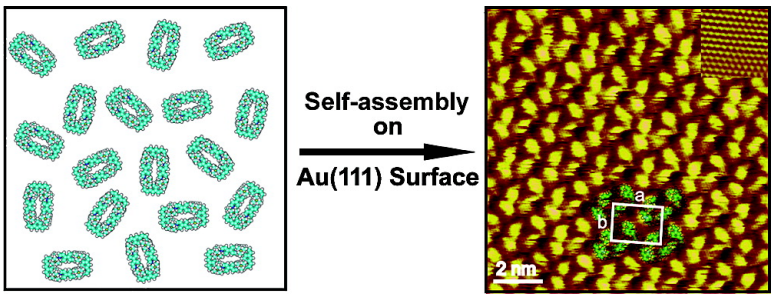

More About This Article

Additional resources and features associated with this article are available within the HTML version:

- Supporting Information
- Links to the 24 articles that cite this article, as of the time of this article download
- Access to high resolution figures
- Links to articles and content related to this article
- Copyright permission to reproduce figures and/or text from this article

View the Full Text HTML

J|A|C|S
ARTICLES
Published on Web 10/28/2005

Self-Organization of a Self-Assembled Supramolecular Rectangle, Square, and Three-Dimensional Cage on Au(111) Surfaces

Qun-Hui Yuan,[†] Li-Jun Wan,*[,†] Hershel Jude,[‡] and Peter J. Stang*[,‡]

Contribution from the Institute of Chemistry, Chinese Academy of Sciences, Beijing, China 100080, and Department of Chemistry, University of Utah, 315 South 1400 East, Salt Lake City, Utah 84112

Received July 22, 2005; E-mail: wanlijun@iccas.ac.cn; stang@chem.utah.edu

Abstract: The structure and conformation of three self-assembled supramolecular species, a rectangle, a square, and a three-dimensional cage, on Au(111) surfaces were investigated by scanning tunneling microscopy. These supramolecular assemblies adsorb on Au(111) surfaces and self-organize to form highly ordered adlayers with distinct conformations that are consistent with their chemical structures. The faces of the supramolecular rectangle and square lie flat on the surface, preserving their rectangle and square conformations, respectively. The three-dimensional cage also forms well-ordered adlayers on the gold surface, forming regular molecular rows of assemblies. When the rectangle and cage were mixed together, the assemblies separated into individual domains, and no mixed adlayers were observed. These results provide direct evidence of the noncrystalline solid-state structures of these assemblies and information about how they self-organize on Au(111) surfaces, which is of importance in the potential manufacturing of functional nanostructures and devices.

Introduction

Self-assembly[1] and self-organization[2] are natural and spontaneous processes that are of ever increasing importance in chemistry and material science. These processes depend on both intermolecular and molecule/substrate interactions. Self-assembly also plays an important role in the "bottom-up" strategy used in nanofabrication and is considered to be a promising supplement to microfabrication.[3−8] Considerble effort has been made to distribute and/or arrange molecules into thin films or on surfaces, with the expectation that the new fabricated film or surface will possess beneficial properties.[9−18] However, it is well known that the performance and functionality of a microfabricated device designed on a solid surface are dependent on the molecular substrate as well as a defined adlayer.[14−20]

Supramolecular assemblies, which make use of dative metal−ligand bonding (e.g., Pt−N or Pd−N),[21−26] exhibit ample functionality. A wide variety of aesthetically pleasing structures have been prepared, from simple parallelograms (e.g., rectangles, triangles, squares, etc.)[27−36] to complicated three-dimensional

[†] Chinese Academy of Sciences.
[‡] University of Utah.

(1) Lehn, J.-M. *Proc. Natl. Acad. Sci. U.S.A.* **2002**, *99*, 4763−4768.
(2) Whitesides, G. M.; Boncheva, M. *Proc. Natl. Acad. Sci. U.S.A.* **2002**, *99*, 4769−4774.
(3) Gimzewski, J. K.; Joachim, C. *Science* **1999**, *283*, 1683−1688.
(4) Lehn, J. M. *Supramolecular Chemistry: Concepts and Perspectives*; VCH: New York, 1995.
(5) Atwood, J. L.; Davies, J. E. D.; MacNicol, D. D.; Vögtle, F.; Lehn, J. M. *Comprehensive Supramolecular Chemistry*; Pergamon: New York, 1996; Vol. 9.
(6) Kolb, D. M. *Angew. Chem., Int. Ed.* **2001**, *40*, 1162−1181.
(7) Gates, B. D.; Xu, Q. B.; Stewart, M.; Ryan, D.; Willson, C. G.; Whitesides, G. M. *Chem. Rev.* **2005**, *105*, 1171−1196.
(8) De Feyter, S.; De Schryver, F. C. *J. Phys. Chem. B* **2005**, *109*, 4290−4302.
(9) Scudiero, L.; Barlow, D. E.; Mazur, U.; Hipps, K. W. *J. Am. Chem. Soc.* **2001**, *123*, 4073−4080.
(10) Yoshimoto, S.; Suto, K.; Tada, A.; Kobayashi, N.; Itaya, K. *J. Am. Chem. Soc.* **2004**, *126*, 8020−8027.
(11) Dinolfo, P. H.; Hupp, J. T. *Chem. Mater.* **2001**, *13*, 3113−3125.
(12) Slone, R. V.; Benkstein, K. D.; Belanger, S.; Hupp, J. T.; Guzei, I. A.; Rheingold, A. L. *Coord. Chem. Rev.* **1998**, *171*, 221−243.
(13) Keffe, M. H.; Benkstein, K. D.; Hupp, J. T. *Coord. Chem. Rev.* **2000**, *205*, 201−228.
(14) Hipps, K. W.; Scudiero, L.; Barclow, D. E.; Cooke, M. P., Jr. *J. Am. Chem. Soc.* **2002**, *124*, 2126−2127.
(15) Barth, J. V.; Weckesser, J.; Cai, C.; Günter, P.; Bürgi, L.; Jeandupeux, O.; Kern, K. *Angew. Chem., Int. Ed.* **2000**, *39*, 1230−1234.
(16) Otsuki, J.; Nagamine, E.; Kondo, T.; Iwasaki, K.; Asakawa, M.; Miyake, K. *J. Am. Chem. Soc.* **2005**, *127*, 10400−10405.
(17) Menozzi, E.; Pinalli, R.; Speets, E. A.; Ravoo, B. J.; Dalcanale, E.; Reinhoudt, D. N. *Chem. Eur. J.* **2004**, *10*, 2199−2206.
(18) Milic, T.; Garno, J. C.; Batteas, J. D.; Smeureanu, G.; Drain, C. M. *Langmuir* **2004**, *20*, 3974−3983.
(19) Han, M. J.; Wan, L. J.; Lei, S. B.; Li, H. M.; Fan, X. L.; Bai, C. L.; Li, Y. L.; Zhu, D. B. *J. Phys. Chem. B* **2004**, *108*, 965−970.
(20) Yoshimoto, S.; Honda, Y.; Murata, Y.; Murata, M.; Komatsu, K.; Ito, O.; Itaya, K. *J. Phys. Chem. B* **2005**, *109*, 8547−8550.
(21) Ruben, M.; Rojo, J.; Romero-Salguero, F. J.; Uppadine, L. H.; Lehn, J. M. *Angew. Chem., Int. Ed.* **2004**, *43*, 3644−3662.
(22) Piguet, C.; Bernardinelli, G.; Hopfgartner, G. *Chem. Rev.* **1997**, *97*, 2005−2062.
(23) Leininger, S.; Olenyuk, B.; Stang, P. J. *Chem. Rev.* **2000**, *100*, 853−908.
(24) Eddaoudi, M.; Moler, D. B.; Li, H. L.; Chen, B. L.; Reineke, T. M.; O'Keeffe, M.; Yaghi, O. M. *Acc. Chem. Res.* **2001**, *34*, 319−330.
(25) Seidel, S. R.; Stang, P. J. *Acc. Chem. Res.* **2002**, *35*, 972−983.
(26) Schalley, C. A.; Lützen, A.; Albrecht, M. *Chem. Eur. J.* **2004**, *10*, 1072−1080.
(27) Yue, N. L. S.; Jennings, M. C.; Puddephatt, R. J. *Inorg. Chem.* **2005**, *44*, 1125−1131.
(28) Martin-Redondo, M. P.; Scoles, L.; Sterenberg, B. T.; Udachin, K. A.; Carty, A. J. *J. Am. Chem. Soc.* **2005**, *127*, 5038−5039.
(29) Cotton, F. A.; Murillo, C. A.; Wang, X.; Yu, R. *Inorg. Chem.* **2004**, *43*, 8394−8403.
(30) Caskey, D. C.; Shoemaker, R. K.; Michl, J. *Org. Lett.* **2004**, *6*, 2093−2096.
(31) Forniés, J.; Gómez, J.; Lalinde, E.; Moreno, M. T. *Chem. Eur. J.* **2004**, *10*, 888−898.

polyhedra (e.g., tetrahedrons, cubes, dodecahedron, etc.).[25,37−43] Possessing magnetic, photophysical, electronic, and/or redox properties that may not be accessible from purely organic systems, these metallamacrocyclic supramolecular assemblies are ideal building blocks for constructing molecular nanodevices.[11,43−49] Fabricating desirable and stable devices from these assemblies on solid surfaces and understanding the rules governing their self-organization on solid supports are significant fundamental steps toward realizing useful nanodevices and nanostructures.[50]

Scanning tunneling microscopy (STM) has proven to be a powerful tool for characterizing supramolecular self-assemblies on surfaces, formed via self-organization.[51−53] From high-resolution images, the stability of the adlayer can be assessed,[54] and details about its structure can be determined, including proximity of the nearest molecule as well as the orientation and conformation of the assembly on the surface.[55−66] For example, the electronic and magnetic properties of [2×2] grid-type Zn(II) and Co(II) complexes on highly oriented pyrolytic graphite (HOPG) have been investigated.[55,56] The orientation of the assembly on HOPG could be tuned by making subtle changes (e.g., addition of a methyl group) in the complexes.[55] Kurth and co-workers[57] were able to prepare straight chains of a supramolecular coordination complex on HOPG using long alkyl chains as a template.

We recently reported the self-organization of a supramolecular rectangle, [(1,8-bis(*trans*-Pt(PEt_3)$_2$)anthracene)(1,4′-bis(4-ethynylpyridyl)benzene)](PF_6)$_4$, on HOPG and Au(111) surfaces.[65] The orientation of the rectangular adlayers was dependent on the surface, demonstrating the importance of molecule/molecule and molecule/substrate interactions in nanofabrication. In this article, we report the STM images obtained from three supramolecular metallamacrocyclic self-assemblies, a small rectangle,[67,68] a square,[69] and a three-dimensional cage[70] (Figure 1), on Au(111) surfaces. The assemblies spontaneously self-organize on Au(111) and form well-ordered two-dimensional adlayers. High-resolution STM images clearly show the arrangement of the assemblies on the surfaces.

Results and Discussion

Supramolecular Rectangle [(1,8-Bis(*trans*-Pt(PEt_3)$_2$)anthracene)(4,4′-bpy)]$_2$(PF_6)$_4$. The chemical structure and space-filling model of the supramolecular rectangle are shown in Figure 1A. From the large-scale STM image (Figure 2A), it can be seen that the rectangle adsorbs on the Au(111) surface and forms an ordered molecular adlayer. The molecular network extends over the atomically flat terrace of Au(111) surface (>100 nm × 100 nm) as a single domain, with only minor molecular defects. The stable adlayer consists of regular molecular rows of the rectangles, aligned along the **A** and **B** directions. The perpendicular rows cross, forming a 90 ± 2° angle. Although a reconstructed Au(111) surface with herringbone lines can be seen in the STM image, it has no effect on forming the defined molecular adlayer.

A high-resolution STM image of the rectangle (Figure 2B) reveals the structural detail of the rectangular adlayer. The molecules appear as sets of four bright spots, which correspond to a supramolecular rectangle, with dimensions of 2.0 nm × 1.2 nm, consistent with the size of the rectangle previously determined from single-crystal X-ray crystallography.[68] The supramolecular rectangle lies flat on the Au(111) surface, with its molecular plane parallel to the Au(111) surface, and a dark depression is seen in the center of each rectangle.

To determine the crystalline relationship between the adlayer and substrate, the underlying Au(111) lattice was observed by scanning the electrode potential to the hydrogen adsorption region where the rectangular adlayer desorbs from the Au(111) surface. A STM image of the underlying surface is shown in the inset in the upper right corner of Figure 2B, showing the

(32) Lee, S. J.; Kim, J. S.; Lin, W. *Inorg. Chem.* **2004**, *43*, 6579−6588.
(33) Kumazawa, K.; Yamanoi, Y.; Yoshizawa, M.; Kusukawa, T.; Fujita, M. *Angew. Chem., Int. Ed.* **2004**, *43*, 5936−5940.
(34) Angaridis, P.; Berry, J. F.; Cotton, F. A.; Murillo, C. A.; Wang, X. *J. Am. Chem. Soc.* **2003**, *125*, 10327−10334.
(35) Kryschenko, Y. K.; Seidel, S. R.; Arif, A. M.; Stang, P. J. *J. Am. Chem. Soc.* **2003**, *125*, 5193−5198.
(36) Qin, Z.; Jennings, M. C.; Puddephatt, R. J. *Inorg. Chem.* **2002**, *41*, 3967−3974.
(37) Alvarez, S. *J. Chem. Soc., Dalton Trans.* **2005**, 2209−2233.
(38) Ke, Y. X.; Collins, D. J.; Zhou, H. C. *Inorg. Chem.* **2005**, *44*, 4154−4156.
(39) Fujita, M.; Tominaga, M.; Hori, A.; Therrien, B. *Acc. Chem. Res.* **2005**, *38*, 369−378.
(40) Reger, D. L.; Semeniuc, R. F.; Smith, M. D. *Inorg. Chem.* **2003**, *42*, 8137−8139.
(41) Radhakrishnan, U.; Schweiger, M.; Stang, P. J. *Org. Lett.* **2001**, *3*, 3141−3143.
(42) Kuehl, C. J.; Yamamoto, T.; Seidel, S. R.; Stang, P. J. *Org. Lett.* **2002**, *4*, 913−915.
(43) Holliday, B. J.; Mirkin, C. A. *Angew. Chem., Int. Ed.* **2001**, *40*, 2022−2043.
(44) Fujita, M. *Chem. Soc. Rev.* **1998**, *27*, 417−425.
(45) Schwab, P. F. H.; Levin, M. D.; Michl, J. *Chem. Rev.* **1999**, *99*, 1863−1933.
(46) Cotton, F. A.; Lin, C.; Murillo, C. A. *Proc. Natl. Acad. Sci. U.S.A.* **2002**, *99*, 4810−4813.
(47) Eddaoudi, M.; Kim, J.; Vodak, D.; Sudik, A.; Wachter, J.; O'Keffe, M. *Proc. Natl. Acad. Sci. U.S.A.* **2002**, *99*, 4900−4904.
(48) Pirondini, L.; Bertolini, F.; Cantadori, B.; Ugozzoli, F.; Massera, C.; Dalcanale, E. *Proc. Natl. Acad. Sci. U.S.A.* **2002**, *99*, 4911−4915.
(49) Würthner, F.; You, C.-C.; Saha-Möller, C. R. *Chem. Soc. Rev.* **2004**, *33*, 133−146.
(50) Stupp, S. I., Guest Editor. Thematic Issue: Functional Nanostructures. *Chem. Rev.* **2005**, *105*, 1023−1562.
(51) Pan, G.-B.; Liu, J.-M.; Zhang, H.-M.; Wan, L.-J.; Zheng, Q.-Y.; Bai, C.-L. *Angew. Chem., Int. Ed.* **2003**, *42*, 2747−2751.
(52) Merz, L.; Guntherodt, H.; Scherer, L. J.; Constable, E. C.; Housecroft, C. E.; Neuburger, M.; Hermann, B. A. *Chem. Eur. J.* **2005**, *11*, 2307−2318.
(53) Miyake, K.; Yasuda, S.; Harada, A.; Sumaoka, J.; Komiyama, M.; Shigekawa, H. *J. Am. Chem. Soc.* **2003**, *125*, 5080−5085.
(54) Xu, X. M.; Zhong, H. P.; Zhang, H. M.; Mo, Y. R.; Xie, Z. X.; Long, L. S.; Zheng, L. S.; Mao, B. W. *Chem. Phys. Lett.* **2004**, *386*, 254−258.
(55) Semenov, A.; Spatz, J. P.; Moller, M.; Lehn, J.-M.; Sell, B.; Schubert, D.; Weidl, C. H.; Schubert, U. S. *Angew. Chem., Int. Ed.* **1999**, *38*, 2547−2550.
(56) Ziener, U.; Lehn, J. M.; Mourran, A.; Möller, M. *Chem. Eur. J.* **2002**, *8*, 951−957.
(57) Kurth, D. G.; Severin, N.; Rabe, J. P. *Angew. Chem., Int. Ed.* **2002**, *41*, 3681−3683.
(58) Xu, Q. M.; Zhang, B.; Wan, L. J.; Wang, C.; Bai, C. L.; Zhu, D. B. *Surf. Sci.* **2002**, *517*, 52−58.
(59) Shieh, D. L.; Shiu, K. B.; Lin, J. L. *Surf. Sci.* **2004**, *548*, L7−L12.
(60) Figgemeier, E.; Merz, L.; Hermann, B. A.; Zimmermann, Y. C.; Housecroft, C. E.; Guntherodt, H. J.; Constable, E. C. *J. Phys. Chem. B* **2003**, *107*, 1157−1162.
(61) Takaishi, S.; Miyasaka, H.; Sugiura, K.; Yamashita, M.; Matsuzaki, H.; Kishida, H.; Okamoto, H.; Tanaka, H.; Marumoto, K.; Ito, H.; Kuroda, S.; Takami, T. *Angew. Chem., Int. Ed.* **2004**, *43*, 3171−3175.
(62) Zell, P.; Mögele, F.; Ziener, U.; Rieger, B. *Chem. Commun.* **2005**, 1294−1296.
(63) Kakegawa, N.; Hoshino, N.; Matsuoka, Y.; Wakabayashi, N.; Nishimura, S. I.; Yamagishi, A. *Chem. Commun.* **2005**, 2375−2377.
(64) Safarowsky, C.; Merz, L.; Rang, A.; Broekmann, P.; Hermann, B. A.; Schalley, C. A. *Angew. Chem., Int. Ed.* **2004**, *43*, 1291−1294.
(65) Gong, J. R.; Wan, L. J.; Yuan, Q. H.; Bai, C. L.; Jude, H.; Stang, P. J. *Proc. Natl. Acad. Sci. U.S.A.* **2005**, *102*, 971−974.
(66) Mourran, A.; Ziener, U.; Möller, M.; Breuning, E.; Ohkita, M.; Lehn, J. M. *Eur. J. Inorg. Chem.* **2005**, 2641−2647.
(67) Kuehl, C. J.; Mayne, C. L.; Arif, A. M.; Stang, P. J. *Org. Lett.* **2000**, *2*, 3727−3729.
(68) Kuehl, C. J.; Songping, D. H.; Stang, P. J. *J. Am. Chem. Soc.* **2001**, *123*, 9634−9641.
(69) Stang, P. J.; Cao, D. H.; Saito, S.; Arif, A. M. *J. Am. Chem. Soc.* **1995**, *117*, 6273−6283.
(70) Kuehl, C. J.; Kryschenko, Y. K.; Radhakirshnan, U.; Seidel, S. R.; Huang, S. D.; Stang, P. J. *Proc. Natl. Acad. Sci. U.S.A.* **2002**, *99*, 4932−4936.

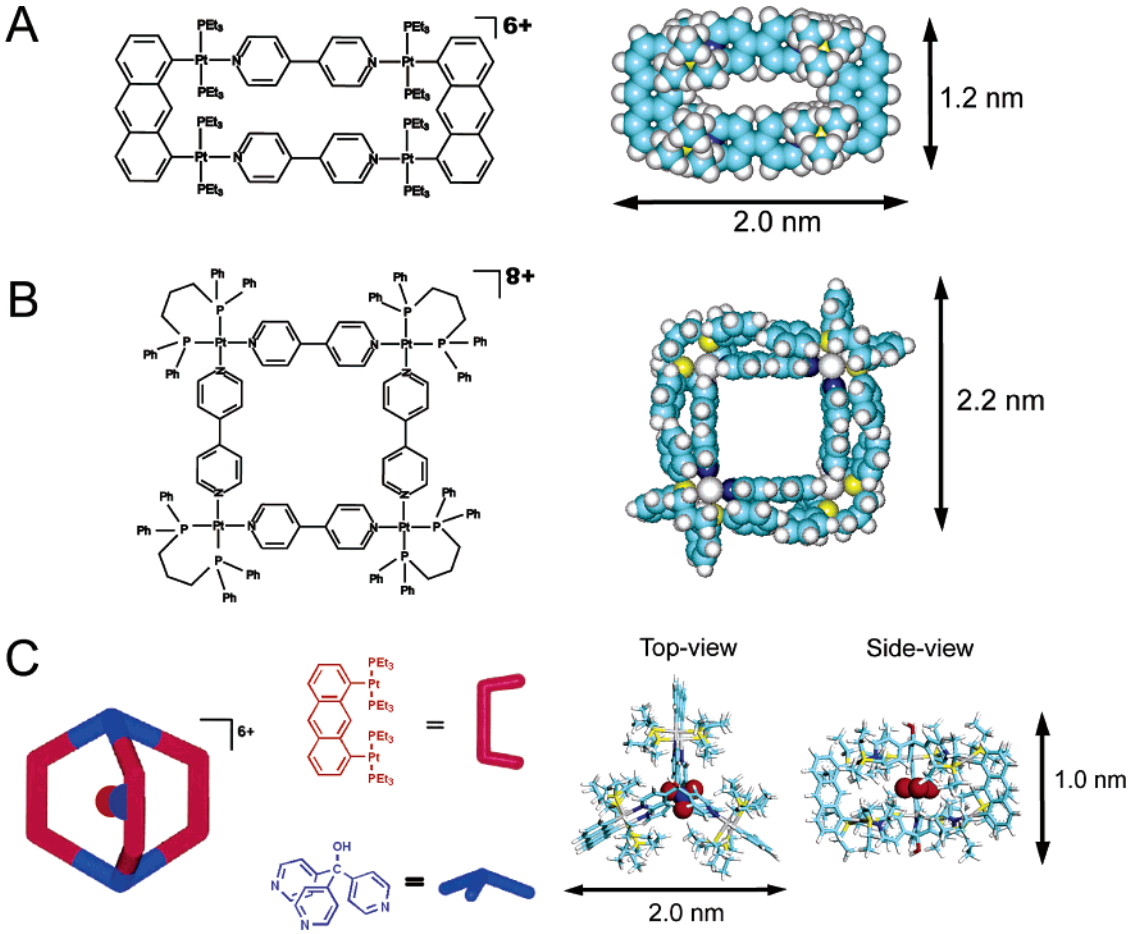

Figure 1. Chemical structure and space-filling/ball-and-stick model of (A) the self-assembled rectangle, (B) the square, and (C) the three-dimensional cage.

Au(111)-(1×1) lattice. Each bright spot corresponds to a gold atom, with an interatomic distance of 0.29 nm, consistent with the crystal parameter of Au(111). The molecular rows of the adlayer, **A** and **B**, align along the ⟨110⟩ and ⟨121⟩ directions of the underlying lattice, respectively. The intermolecular distances in the rows were measured to be $a = 2.0$ nm and $b = 1.5$ nm. From the adlayer symmetry and the intermolecular distance, the structure of the adlayer can be defined as a $(7 \times 3\sqrt{3})$ structure. The long edge of the supramolecular rectangle aligns along the **A**−**A′** direction (Figure 2C), and it deviates by approximately 30 ± 2° from the underlying Au(111)-[110] close-packed direction. A unit cell is described in Figure 2B.

A structural model is proposed in Figure 2C. For simplicity, the ⟨110⟩ and ⟨121⟩ directions of the gold lattice are referred to as I and II, respectively. The **A**−**A′** direction is defined as the long edge of a supramolecular rectangle. The rectangle lies flat on the Au(111) surface, preserving its shape. The orientation of the rectangle forms a 30° angle with the ⟨110⟩ direction of the Au(111) lattice (Figure 2C). A close-packed array is self-organized with strong molecule/molecule and molecule/substrate interactions. The molecular rows cross each other, forming a 90° angle. However, due to the large size and complicated chemical structures of the assembly, it is difficult to determine the exact interactions that stabilize the molecular adlayers. For these reasons, we have proposed a simplified model which shows only the molecular organization of the assemblies on the surface, such as those used to describe porphyrin and phthalocyanine complexes on Au(111) surfaces.[14,71] This model is in good agreement with the observed STM images.

Comparing the present rectangle with the larger supramolecular rectangle previously reported,[65] it is seen that both molecules adsorb on Au(111) and self-organize into ordered, close-packed arrays while preserving the rectangular structure. Both rectangles lie flat on the Au(111) surface, and no decomposition has been observed. The large rectangle also adsorbs onto HOPG surfaces and forms an ordered self-organized adlayer. However, all attempts to observe the small rectangle on HOPG were unsuccessful, suggesting that the large rectangle has stronger interactions between the molecule and the underlying HOPG substrate, resulting in more stable molecular architectures. Presumably, the differences in the size of the molecules are responsible for the different symmetry and parameters of the two systems.

Supramolecular Square $[Pt(dppp)(4,4'\text{-bpy})]_4(CF_3SO_3)_8$. The chemical structure and a space-filling model of the supramolecular square are shown in Figure 1B. Along one diagonal of the square, the PPh_2 groups point out, extending the size of the square, while along the other diagonal they point inward. A large-scale STM image (50 nm × 50 nm) of the molecular adlayer is shown in Figure 3A. The squares self-organize onto the surface of the Au(111) substrate, and an area of 50 nm × 50 nm is covered with a well-ordered array of the

(71) Yoshimoto, S.; Higa, N.; Itaya, K. *J. Am. Chem. Soc.* **2004**, *126*, 8540−8545.

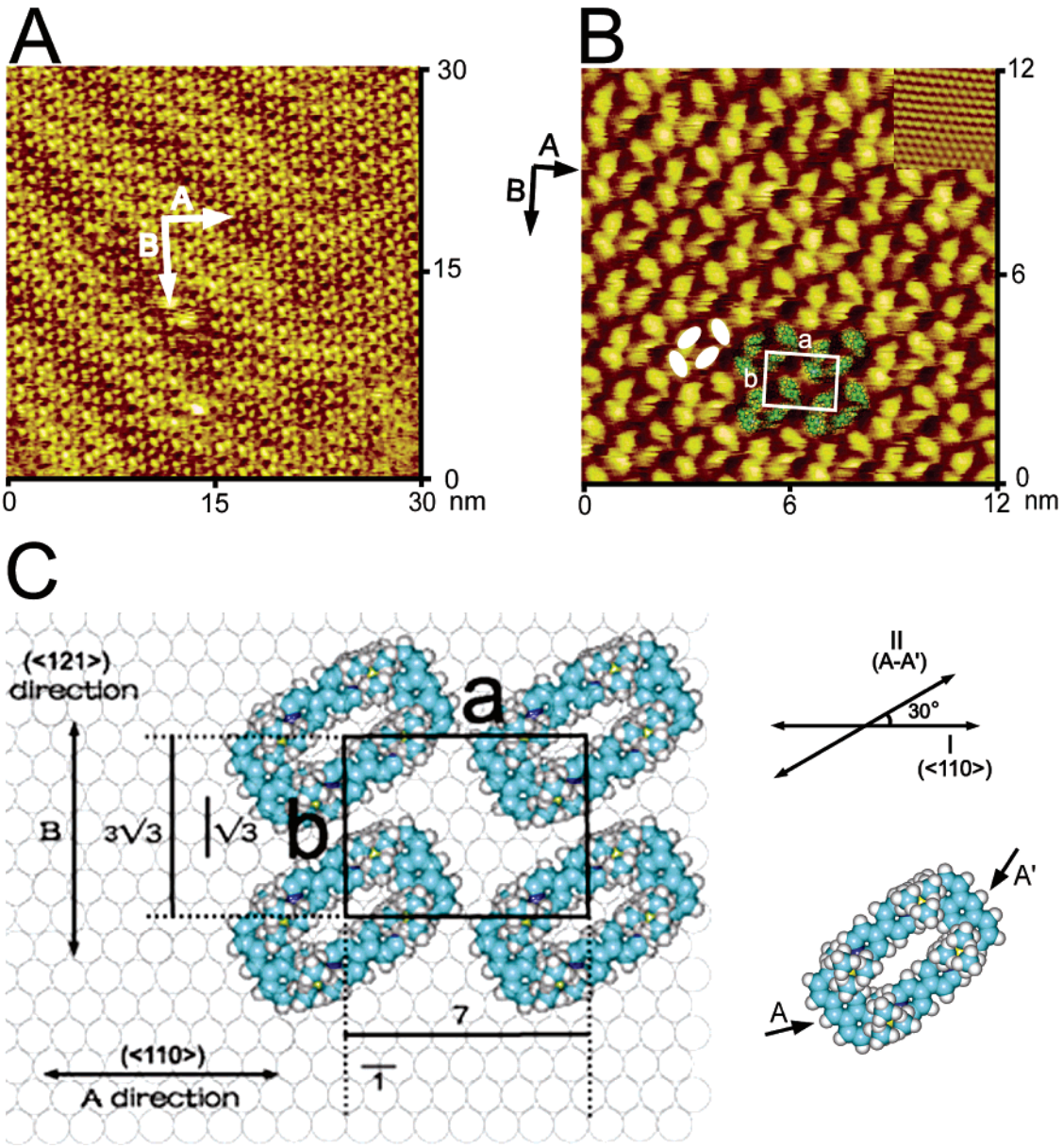

Figure 2. (A) Large-scale STM image ($E = 550$ mV, $E_{tip} = 392$ mV, $I_{tip} = 941.0$ pA) of the self-assembled rectangles adsorbed on a Au(111) surface. (B) High-resolution STM image ($E = 550$ mV, $E_{tip} = 370$ mV, $I_{tip} = 765.0$ pA) of the rectangular adlayer and showing the underlying Au(111)-(1×1) lattice in the upper right corner. (C) Proposed structural model for the adlayer.

assemblies.The rows of squares extending in the **A** and **B** directions (Figure 3A) cross, forming a 90° angle. The rectangle forms much nicer and larger adlayers than the square. The size of the rectangular adlayers is routinely larger than 100 nm × 100 nm, while adlayers of this size, which are void of defects, are rarely observed for the square. This phenomenon may be due to the more complicated stereoscopic conformation of the supramolecular squares.

From the high-resolution STM image (Figure 3B), the internal structure, molecular orientation, and packing arrangement of the adlayer are visible. Compared to the underlying Au(111) lattice shown as an inset in the upper right corner of Figure 3B, the molecular rows in the **A** and **B** directions are found to be parallel to the ⟨110⟩ and ⟨121⟩ directions, respectively. Individual molecules can easily be identified from the STM image due to the structure of the molecular assembly, and one square in the image corresponds to a supramolecular square. Each square has a dark depression in the center (Figure 3B). The size of a square was determined to be 2.1 ± 0.1 nm, consistent with the size determined from the previously reported single-crystal X-ray structure.[69] Along **A** there is a periodic intermolecular distance of 2.3 ± 0.1 nm, while along **B** it is 2.5 ± 0.1 nm. Therefore, a unit cell defined as an $(8 \times 5\sqrt{3})$ structure is superimposed on the STM image in Figure 3B. As observed in the space-filling model, the PPh_2 groups can be seen in the high-resolution STM image (Figure 3B). Although the molecule has a stereoscopic conformation, the STM image shows that each molecule absorbs on the surface with its molecular plane parallel to the substrate. Similar to the supramolecular rectangle, the edge of the square forms a 15° angle with the ⟨110⟩ direction of the underlying Au(111) lattice. In this arrangement, the squares form a close-packed adlayer on the Au(111) surface. A structural model for the self-organization of the square on Au(111) surfaces is proposed in Figure 3C. It can be seen that

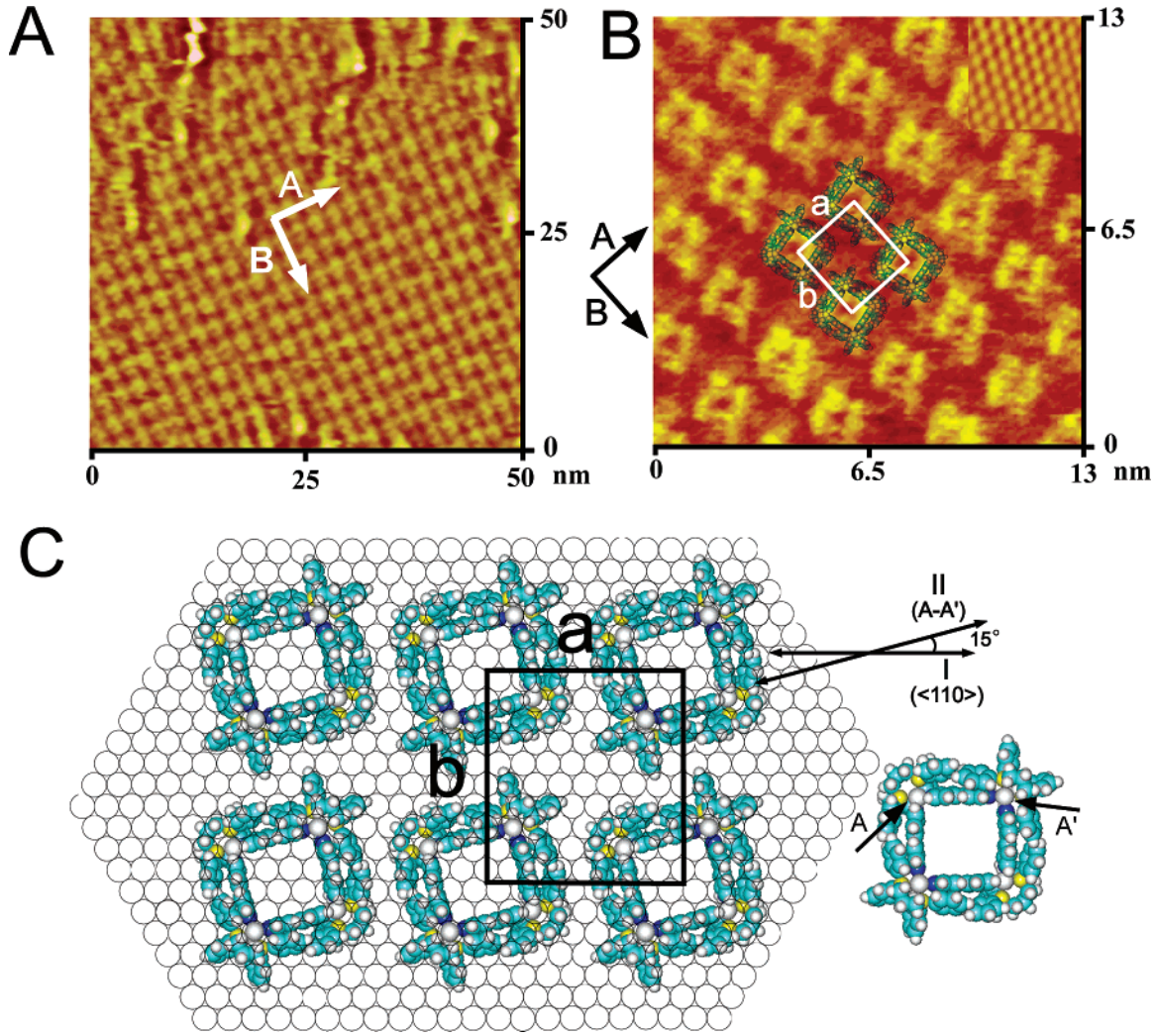

Figure 3. (A) Large-scale STM image (E = 510 mV, E_{tip} = 281 mV, I_{tip} = 966.3 pA) of the self-assembled squares adsorbed on a Au(111) surface. (B) High-resolution STM image (E = 510 mV, E_{tip} = 195 mV, I_{tip} = 531.8 pA) of the adlayer and showing the underlying Au(111)-(1×1) lattice in the upper right corner. (C) Proposed structural model for the adlayer.

each molecule sits on the substrate with its edge deviating by approximately 15° from the ⟨110⟩ direction.

Schalley and co-workers[64] have reported STM images of a self-assembled square, $[Pt(en)(4,4'\text{-bpy})]_4(NO_3)_8$ (en = ethylenediamine, 4,4′-bpy = 4,4′-bipyridine), on a Cu(100) surface modified with a chloride adsorbate layer. The negatively charged chloride layer causes the cationic square to adsorb and lies flat on the negatively charged surface. However, due to the acidic conditions used to prepare the surface, the square slowly opens and chainlike oligomers coadsorb with the square. The authors also reported preliminary experiments performed on HOPG for the ethylenediamine square as well as the $[Pt(dppp)(4,4'\text{-bpy})]_4(CF_3SO_3)_8$ square, which we report here on Au(111). Under the conditions used to deposit the square (solution casting) and to record the images, the squares showed a striped pattern in the STM images. From these data, it was concluded that intermolecular interactions dominate over molecule/substrate interactions on neutral graphite surfaces. We also tried to record STM images of the square on HOPG; however, no ordered monolayers were observed. Comparison of our results on a Au(111) surface with those of Schalley and co-workers[64] on Cu(100) and HOPG demonstrates the importance of judiciously choosing both the surface and conditions used in the self-organization process.

Three-Dimensional Cage [(Tris(4-pyridyl)methanol)$_2$(1,8-bis(*trans*-Pt(PEt$_3$)$_2$)anthracene)$_3$](PF$_6$)$_5$(NO$_3$). The chemical structure as well as a ball-and-stick model of the three-dimensional cage is shown in Figure 1C. The structure of this assembly is complicated, and the model as viewed from the side and top is shown. From the top, the cage has a three-blade propeller shape, while it looks like a rectangle when viewed from the side. The cage adsorbs onto the surface of Au(111) and forms a large-scale STM image (30 nm × 30 nm). It can be seen that the assemblies self-organize into a well-ordered two-dimensional array with regular molecular rows (Figure 4A). The structural details of the supramolecular cage adlayer can be seen in the high-resolution STM images (Figure 4B).

It can be seen that the adlayer consists of regular molecular rows which are labeled **A** and **B**. In both directions, the molecular rows are clear, and the arrangement of the molecules is visible. The three-dimensional cage consists of a set of nine bright spots. In the molecular model (Figure 4C), the bright spots have been separated into subsets of three spots, which

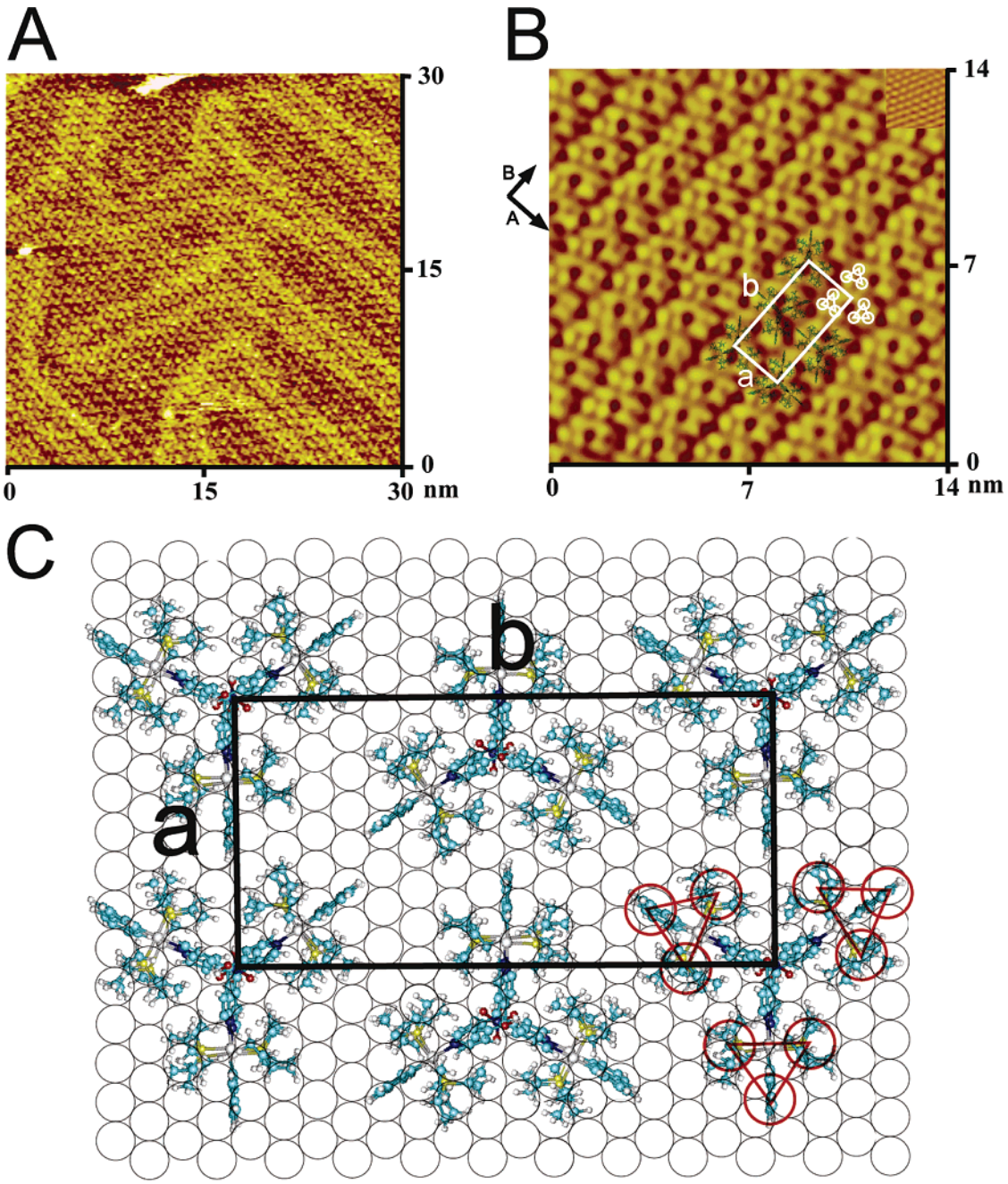

Figure 4. (A) Large-scale STM image (E = 550 mV, E_{tip} = 312 mV, I_{tip} = 1.000 nA) of the self-assembled three-dimensional cage on a Au(111) surface. (B) High-resolution STM image (E = 550 mV, E_{tip} = 337 mV, I_{tip} = 852.1 pA) of the adlayer and showing the underlying Au(111)-(1×1) lattice in the upper right corner. (C) Proposed structural model for the adlayer.

corresponds to one "propeller". These details are emphasized for clarity in Figure 4B by sets of white circles. Each subset of three spots forms a triangle. The length between the two corners of a propeller is measured to be 2.0 ± 0.1 nm, in agreement with the X-ray crystallographic data.[70]

On the surface of Au(111), the cage molecules are ordered so that all three "blades" point in the same direction along **A**. However, the molecules are interdigitated along **B**, with all three blades of a neighboring molecule pointing in the opposite direction. This arrangement of cages results in one "blade" pointing along **A**. From the underlying Au(111) lattice shown in the inset in Figure 4B, rows **A** and **B** are found to be parallel to the ⟨110⟩ and ⟨121⟩ directions, respectively. The intermolecular distances along the directions **A** and **B** are 2.0 ± 0.1 and 4.0 ± 0.1 nm, respectively. According to the intermolecular distances and the orientation of the adlayer relative to the underlying Au(111) lattice, a unit cell is outlined in Figure 4B. The adlayer can be defined as a $(7 \times 8\sqrt{3})$ structure.

On the basis of the above analysis, a schematic model can be constructed for the supramolecular adlayer on a Au(111) surface in Figure 4C. The cages stand on the gold surface, in an arrangement consistent with the top view model in Figure 3B. The three blades in a propeller are in contact with the substrate surface, with the cages standing on their end. The

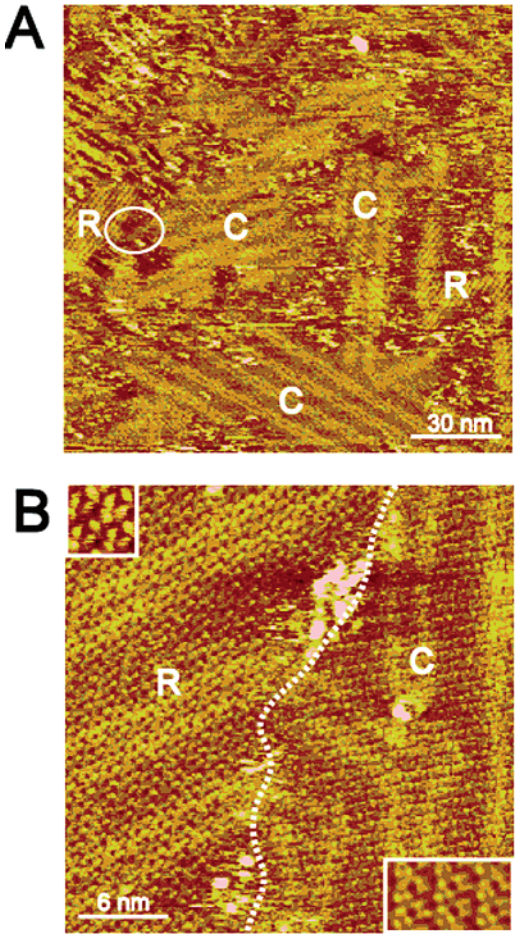

Figure 5. (A) Large-scale STM image ($E = 550$ mV, $E_{tip} = 370$ mV, $I_{tip} = 900.0$ pA) of a rectangle/cage mixed adlayer on a Au(111) surface. (B) Magnified image of the area inside the circle in part A, showing high-resolution images of rectangular (upper left) and three-dimensional cage (lower right) adlayers.

proposed structural model is consistent with what is revealed by high-resolution STM images.

Mixed Adlayers of Supramolecular Rectangles and Three-Dimensional Cages. Recently, surfaces on which multiple components self-organize to form intact and stable adlayers are receiving increased attention due to their possible applications in nanoscience and nanotechnology.[14,20,51,72] Through self-organization, multiple components could be layered on a surface with precise geometry and function. For example, the intermolecular distance and assembly pattern in a self-organization were tuned by using molecules with different lengths of alkyl chains.[73,74] After observation of the self-assemblies with individual supramolecular rectangles, squares, and cages, a binary component system was prepared consisting of the supramolecular rectangle and three-dimensional cage, and the resulting surface was investigated by STM.

Figure 5A is a large-scale STM image of the mixed rectangle/cage adlayer on a Au(111) surface. The surface is covered with the assemblies, which self-organize into individual domains. The rectangle domains are marked with an R and the cage domains are marked with a C. The area within the circle in Figure 5A is magnified in Figure 5B. The rectangle and cage domains can be seen, and the boundary of the two domains is marked with white dots. From Figure 5B, it is seen that the molecules form ordered assemblies in the individual domains, although the molecular appearances and direction of the rows in the two domains are different. Most of the defects and molecular clusters appear along the domain boundary. High-resolution STM imaging was used to reveal the molecular details in the two domains. The results are shown in the insets in the upper left and lower right corners of Figure 5B, corresponding to the domains R and C, respectively. In domain R, high-resolution images reveal a rectangular conformation, consistent with the results observed for adlayers consisting only of rectangle assemblies (e.g., Figure 2B). In domain C, the high-resolution STM image shows an arrangement with three-dimensional cages, similar to the results observed in Figure 4B. Although efforts were made to find new organized structures with two components, only the phase-separated organization was observed on the Au(111) surface.

In a binary system, the order of the structure on a surface has three possibilities: (i) phase separation, (ii) preferential adsorption, and (iii) ordered assembly with two molecules. The possibilities are dominated by the interactions between molecules, molecule/substrate interactions, and intramolecular reactions. In the present study, both types of molecules adsorb on the Au(111) surface, resulting in a nonpreferential adsorption. However, the differences in the conformation and symmetry of the two molecules induce a phase separation rather than an ordered uniform assembly. Further studies of mixed assemblies are in progress.

In summary, we have successfully fabricated well-ordered self-organized molecular architectures with three metalla-macrocyclic supramolecular assemblies, a rectangle, a square, and a three-dimensional cage, on a Au(111) surface. The surfaces and the resulting molecular conformations have been investigated with STM. The assemblies preserve their shape and do not decompose on the Au(111) surface. STM imaging provides direct structural evidence for the noncrystalline solid-state structure of these assemblies. The molecules spontaneously adsorb on Au(111) and self-organize into ordered adlayers. The rectangles self-organize into a $(7 \times 3\sqrt{3})$ structure, the square into an $(8 \times 5\sqrt{3})$ structure, and the three-dimensional cages into a $(7 \times 8\sqrt{3})$ structure. The self-organization on Au(111) of a binary component solution containing supramolecular rectangles and cages resulted in a two-phase surface with no new mixed adlayers. By carefully controlling the substrate and coating materials, many new molecular architectures may be fabricated.

Experimental Section

The self-assembled supramolecular assemblies were synthesized as previously described.[67−70] Spectroscopic grade ethanol was purchased from Acros and used as received. Well-defined Au(111) surfaces on single-crystal gold beads were prepared as previously described.[65,75] Before each measurement, the Au(111) electrodes were annealed in a hydrogen−oxygen flame and quenched in hydrogen-saturated ultrapure

(72) Baker, R. T.; Mougous, J. D.; Brackley, A.; Patrick, D. L. *Langmuir* **1999**, *15*, 4884−4891.
(73) Wu, P.; Zeng, Q. D.; Xu, S. D.; Wang, C.; Yin, S. X.; Bai, C. L. *Chemphyschem* **2001**, *2*, 750−754.
(74) Marchenko, A.; Cousty, J.; Van, L. P. *Langmuir* **2002**, *18*, 1171−1175.
(75) Wan, L. J.; Terashima, M.; Noda, H.; Osawa, M. *J. Phys. Chem. B* **2000**, *104*, 3563−3569.

water (Mill-Q, ≥18.2 MΩ, TOC < 5 ppb) to obtain a clean (1 × 1) structure. The gold beads were immediately used for STM measurements.

The self-assembled monolayers were prepared by immersing the gold beads in an ethanol solution (10 μM) of the assembly for 1 min. The mixed rectangle/three-dimensional cage adlayers were formed by immersing the Au(111) beads in an ethanol solution of the assemblies (5 μM rectangle and 5 μM three-dimensional cage) for 1 min, rinsing thoroughly with ultrapure Milli-Q water, and promptly mounting in a Teflon electrochemical cell. The STM images were recorded with a Nanoscope E STM instrument (Digital Instruments) in 0.1 M $HClO_4$ solution (ultrapure grade, Kanto Chemical Co., Japan). Typical potentials used in these experiments were between 510 and 550 mV, where no surface redox reactions occur and the molecular adlayers are preserved. All potentials are reported versus the reversible hydrogen electrode.

The STM experiments were preformed in solution, where the electrolyte solution protects the gold surface from atmospheric contaminants.[10,71] The STM tips were prepared by electrochemically etching (12−15 V) a tungsten wire (0.25 mm in diameter) in 0.6 M KOH until the etching process stopped. The tungsten tips were coated with clear nail polish to minimize Faradaic current. STM images were recorded in constant-current mode with a high-resolution scanner, and without further processing (e.g., high-pass filtering), to evaluate the corrugation heights of the adsorbed molecules. However, a low-pass filter was used in the STM images of the cage to minimize noise. Tunneling conditions are reported in the respective figure captions. Molecular models were built according to the previously reported X-ray crystallographic data with HyperChem 6.0 software (Hypercube, Inc).[68−70] Estimated errors in unit cell parameters *a* and *b* are ±0.2 nm, unless otherwise noted.

Acknowledgment. L.-J.W. thanks the National Natural Science Foundation of China (Nos. 20025308 and 20121301), the National Key Project on Basic Research (Grant G2000077501 and 2002CCA03100), National Center for Nanoscience and Nanotechnology of China, and the Chinese Academy of Sciences for financial support. P.J.S. thanks the NIH (GM-57052) and the NSF (CHE-0306720) for support of this work.

JA0549300